Nanoscale

PAPER

View Article Online
View Journal | View Issue

Cite this: *Nanoscale*, 2025, **17**, 23443

Electronic fingerprints of confined and adsorbed water in SWCNTs

Said Pashayev, [a,b] Romain Lhermerout, [a,c] Christophe Roblin,[a] Eric Alibert,[a] Remi Jelinek,[a] Nicolas Izard,[a] Rasim Jabbarov,[b] Francois Henn[a] and Adrien Noury *[a]

Received 12th May 2025,
Accepted 16th August 2025

DOI: 10.1039/d5nr01939g

rsc.li/nanoscale

This article shows the differentiation between water adsorbed outside of a single-walled carbon nanotube (CNT) and that confined inside. This distinction is made possible by tracking the electronic transport of a CNT-based field effect transistor constructed with an individual nanotube and exposed to controlled environments. The presence of water shifts the electrical neutrality point, indicating charge transfer between the nanotube and its environment. We identify three types of water molecules: (i) chemically adsorbed on the SiO_2 surface, forming silanol groups, (ii) physically adsorbed outside the nanotube, and (iii) confined inside. The first type is eliminated only by high-temperature treatment under vacuum, while the latter two desorb at room temperature under moderate or high vacuum, *i.e.* 10^{-3} mbar. We observe that water confinement inside the nanotube is fast and thermodynamically favorable, with no qualitative influence from the metallicity of the nanotube.

1 Introduction

Counterintuitively, water can spontaneously adsorb inside hydrophobic carbon nanotube (CNT) channels. This occurs because the surface tension of water is lower than the wetting threshold of CNTs,[1] and the chemical potential of water inside a single-walled carbon nanotube (SWCNT) is lower than in bulk water.[2] Confining water within nanoscale channels alters the orientation of water molecules[3] and reduces its dielectric permittivity.[4] Despite these effects, the impact of confined water on the electronic properties of CNTs remains poorly understood. It has been suggested that confined water may modify the internal electric field, potentially polarizing the SWCNT and altering its density of states (DOS).[5]

When studying water adsorption on an individual SWCNT deposited on a SiO_2 substrate, two distinct types of water states can be identified: (i) chemisorbed water, which forms silanol groups at the SiO_2 surface and at the CNT interface, and (ii) physisorbed water, which weakly adsorbs either directly onto the CNT surface or bonds with silanol groups. Physisorbed water can be removed easily by pumping under vacuum at room temperature, while chemisorbed water requires higher temperatures (>200 °C) and secondary vacuum to desorb.[6]

To the best of our knowledge, a clear discrimination of the impact of water confined inside or adsorbed outside is missing. However, such a discrimination is not possible on macroscopic samples, since one may expect the CNT response to water adsorption to be extremely broad when working with a distribution of different diameters. Therefore, it is necessary to investigate the impact of water at the level of an individual CNT.

The intrinsic electronic properties of SWCNTs, such as carrier mobility and neutrality points, as well as their extrinsic properties, like the Schottky barrier between the SWCNT and a metal, are highly sensitive to environmental conditions.[7,8] For instance, exposure of CNT field-effect transistors (CNTFETs) to ambient air leads to hysteretic behavior.[9,10] Similarly, CNTFET conductance has been modified when exposed to various salts. Four possible mechanisms were proposed to account for the modification of the CNT transfer characteristics upon analyte adsorption: electrostatic gating or doping, Schottky barrier modulation, capacitance changes, and variations in charge mobility.[11] Electrostatic gating results from CNT doping by adsorbed molecules, shifting conductance along the gate voltage axis. The adsorbed molecules can also modify the local work function at the CNT–metal interface, tuning the Schottky barrier and affecting the electron and hole conductance branches differently. The capacitance effect arises when adsorbed molecules alter the gate capacitance, changing the

[a]*Laboratoire Charles Coulomb (L2C), Univ Montpellier, CNRS, Montpellier, France. E-mail: adrien.noury@umontpellier.fr*
[b]*Institute of Physics of the Ministry of Science and Education of the Republic of Azerbaijan, Baku, Azerbaijan*
[c]*Univ. Grenoble Alpes, CNRS, LIPhy, 38000 Grenoble, France*

slope of the CNTFET transfer characteristics. Finally, the adsorbed molecules can influence carrier mobility, leading to conductance changes in either or both conductance branches.

Water–electron coupling has been studied in both molecular dynamics (MD) simulations and experiments, primarily focusing on water adsorbed on the outer walls of closed CNTs or CNT networks. In MD studies, it was found that water decreases electrostatic gating, mobility, and capacitance, likely due to doping or capacitance effects between water and the CNT.[12–14] Experimental studies have shown that water adsorption alters the threshold voltage and ON–OFF ratio of CNTs.[15] Furthermore, water exhibits an electron-donating nature when exposed to a network of closed SWCNTs, with semiconducting SWCNT networks showing greater sensitivity than metallic ones.[16] This difference is attributed to the lower DOS near the Fermi level in metallic tubes compared to the valence band edge in semiconducting ones.[17] To summarize, liquid water adsorption on the outside of CNTFETs tends to increase hysteresis and shift gate voltage neutrality points to more negative values, though the exact mechanism of coupling, either doping or capacitance, remains debated.[12,18,19]

In this work, we investigate water interactions with an individual SWCNT-based CNTFET. We measure the effects of water adsorption and confinement by comparing the behavior of the CNTFET when the tube is first closed and then opened, allowing for clear differentiation between the various water states. Our observations show that the shift in the gate voltage neutrality point in the CNT transfer characteristics is primarily driven by doping rather than by capacitance effects. We distinguish three water states: (1) physisorbed water on the CNT exterior, (2) confined water inside the CNT, and (3) chemisorbed water (*e.g.*, silanol groups) at the SiO_2 surface near the CNT. Water adsorption, both outside the CNT and within the nanotube, occurs rapidly (in less than a minute under experimental conditions), while water desorption takes 40–60 minutes and requires vacuum and/or annealing, depending on the adsorption site. This disparity between adsorption and desorption times indicates a significant entropic contribution.[3] Furthermore, we show that the metallicity of the nanotube does not qualitatively affect its interaction with water.

2 Materials and methods

Carbon nanotubes are grown using Chemical Vapor Deposition (CVD) on a Si/SiO_2 wafer, with the SiO_2 layer obtained *via* either dry oxidation (300 nm) or wet oxidation (2 μm). An Fe-based catalyst solution is used for the synthesis.[20] Scanning Electron Microscopy (SEM) is employed to locate an individual SWCNT suitable for use in a FET. The selected nanotube is electrically contacted by depositing titanium and platinum electrodes with 10 nm and 90 nm thicknesses, respectively. A SEM image of the final device is shown in Fig. 1a, which displays metallic electrodes of 5 μm width spaced 5 μm apart, deposited on the SWCNT. A global gate is formed by contacting the doped Si substrate with silver paste.

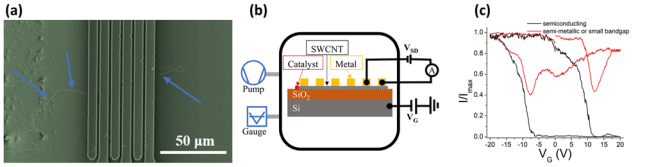

Fig. 1 Device fabrication and characterization: (a) SEM image of a CNTFET. The nanotube (blue arrows) is grown by CVD from the catalyst patterns (visible on the left). Ti and Pt electrodes are deposited on the CNT by E-beam evaporation; (b) customized chamber used to measure the device under a controlled atmosphere; (c) transfer characteristic curves measured for a semiconducting and a semi-metallic or small band gap CNT in air.

The transfer characteristics of the SWCNT-FET are measured in air using a probe station and a source measure unit (SMU). For experiments under a controlled atmosphere or vacuum, a custom-designed chamber (Fig. 1b) is used. The transfer characteristics are measured by sweeping the gate voltage while applying a constant source–drain bias voltage (V_{SD} = 10 mV). Fig. 1c illustrates the typical response of semiconducting (black) and semi-metallic or small band-gap (red) CNTs in air, where hysteresis in the transfer characteristics is observed, indicating charge trapping in the environment (on the substrate, at the substrate–CNT interface, or on the CNT).[21]

To reliably study the impact of water, experiments are conducted on individual SWCNTs by exposing both the outside and the inside of the tubes to water. CVD-grown CNTs have closed ends with fullerene-like caps, requiring intentional end opening to enable water filling. This is accomplished through electrical breakdown, where a voltage is applied between selected electrodes to cut the CNT at a specific location. The resulting current induces Joule heating, which ultimately causes the CNT to fuse between the two electrodes, as evidenced by an abrupt drop in the current–voltage curve (Fig. S1). This procedure is conducted under 10^{-3} mbar vacuum conditions. The ends of the nanotube are thus left open through a process of electrical cutting.[22] A current of 10–50 μA leads to heating the CNT to 1300–1600 K.[23] In this step, we clearly distinguish individual SWCNTs from multi-walled or bundled tubes. When the breakdown current is below 30 μA with a single jump at both ends, the CNT is considered individual (Fig. S1). In what follows, we only focus on individual SWCNTs.

3 Coupling mechanism between electrons and water molecules

In this work, we show that the coupling between electrons and water molecules is primarily dominated by doping, rather than by capacitive effects.

Fig. 2a compares the response of a closed individual SWCNT in air and when soaked in Milli-Q water. We observe that the ON/OFF transition disappears under water. Among the four possible mechanisms reported,[11] only two can explain

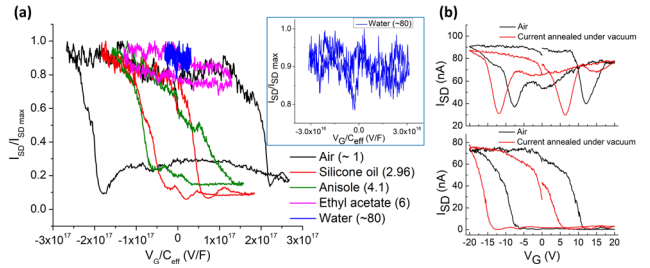

Fig. 2 The transfer characteristic curve of the SWCNT upon exposure to different environments: (a) closed individual SWCNT exposed to liquids with different dielectric constants. Normalized current *versus* gate voltage rescaled by the capacitance formed with different liquids. The inset is a zoom at low V_G/C_{eff} in the case of water; (b) I_{SD} as a function of V_G for two SWCNTs made of either semi-metallic or small bandgap (top) or semiconducting (bottom) individual nanotubes exposed to air (black curves) and after current annealing (T > 1000 K) under vacuum (red curves).

such an outcome: (i) the capacitance effect, where the high dielectric constant of water could rescale the gate axis, effectively shifting the ON/OFF transition, and (ii) doping, where an increase in charge trapping in the CNT environment shifts the neutrality point.

To test the capacitance hypothesis, we soaked the closed CNTFET in non-aqueous liquids with increasing dielectric constants. If the conductance change were purely due to the dielectric constant, a master curve should emerge by rescaling the gate voltage (V_G) axis based on the capacitance, as the CNTFET conductance is proportional to the applied electric field, *i.e.*, $G_{CNT} = f(q_{CNT})$, with $q_{CNT} = C_{eff}V_G$. Here, C_{eff} is the effective gate capacitance, dependent on both the dielectric constant of SiO_2 and the liquid environment, $C_{eff} = g(\varepsilon_{SiO_2}, \varepsilon_r)$, where ε_{SiO_2} is the permittivity of SiO_2 and ε_r is the dielectric constant of the liquid. Numerical simulations provide the exact value of C_{eff} for each liquid, as presented in Table S1. Fig. 2a shows the normalized current *versus* the rescaled gate voltage for the tested liquids. The raw data are also shown in Fig. S2. The normalization facilitates tracking shifts in the gate axis, but the transfer functions do not overlap. This indicates that the dielectric constant of the liquid does not dominate the change in the transfer characteristics, suggesting that doping is the primary mechanism.

To confirm doping as the coupling mechanism, we compare the transfer characteristics of the CNTFET in air and after annealing under secondary vacuum, when the CNT is fully dehydrated. Fig. 2b presents the transfer characteristics of a CNTFET made of individual SWCNTs with different metallicities, exposed to air with 40–50% relative humidity and after current annealing under 10^{-3} mbar vacuum. The key difference between the water-exposed and water-free devices is the shift in the gate voltage neutrality point, regardless of the nanotube's metallicity. This confirms that doping from water molecules is the dominant coupling mechanism. Additionally, doping effects are observed when exposing closed SWCNTs to varying humidity levels (Fig. S3).

4 Differentiating water confined inside from that adsorbed outside the individual SWCNT

We demonstrate that it is possible to differentiate water adsorbed outside from that confined inside by comparing the CNTFET response before and after opening the tube. To measure the impact of water adsorption, we set a reference state for each CNTFET after annealing under vacuum, ensuring that the device is completely dry and minimizing the concentration of silanols on the substrate. Fig. 3a shows the relative change in V_G^+ (corresponding to the neutrality point on the positive side) of closed and opened tubes under various environments: (i) after current annealing under 10^{-3} mbar vacuum, (ii) after about 1 min exposure to ambient air, (iii) after 1 hour exposure to ambient air, and (iv) at room temperature under 10^{-3} mbar. We repeated the exposure cycles several times to ensure reproducibility (Fig. S4).

The main difference between the closed and open cases occurs after placing the CNTFET under 10^{-3} mbar vacuum. While vacuum does not noticeably impact the closed CNTFET, it significantly shifts V_G^+ when the nanotube is open. This shows that the change is due to water confined inside the CNT. The initial increase in V_G^+ when exposed to air, whether the tube is open or closed, can be attributed to doping by water molecules adsorbed outside, either chemically or physically. We also tested the device with helium exposure after vacuum annealing (Fig. S5). The absence of any change in the transfer characteristics confirmed that the observed impact was related to air (oxygen and water molecules).

Exposure to ambient air for 1 hour did not lead to any change in either open or closed cases. This indicates that water adsorption is spontaneous and relatively fast, both outside and inside the CNT. Additionally, when the opened CNTFET was exposed to liquid water and subsequently dried

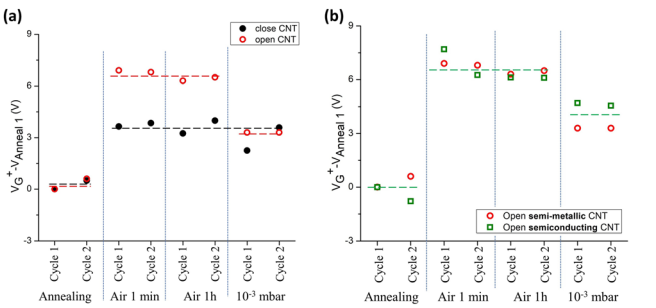

Fig. 3 Differentiating water confined inside from that adsorbed outside an individual SWCNT and the impact of metallicity. Closed and open tubes are represented by filled and open symbols, respectively. Symbols are experimental data; horizontal and vertical dashed lines are guides to the eye. (a) Individual SWCNT exposed to different environments: after current annealing under 10^{-3} mbar vacuum, ~1 min exposure to ambient air, 1 h exposure to ambient air, and under 10^{-3} mbar vacuum at room temperature; (b) comparison of 2 open individual SWCNTs with different metallicities, exposed to the same environments as in (a).

using a nitrogen (N_2) flow, the results showed that exposure to liquid water and its evaporation had the same impact as exposure to ambient air (Fig. S6). This confirms that water, rather than oxygen, dominates the response of the device. Importantly, removing liquid water using a dry N_2 flow is insufficient to desorb water confined inside the tube, highlighting the stable confinement of water within the nanotube. However, under 10^{-3} mbar vacuum, the closed CNTFET exhibited no significant change, whereas the open CNTFET displayed a significant shift in the gate voltage neutrality point. This shift can be attributed to the desorption of confined water.

Finally, both open and closed tubes returned to their initial states after annealing under vacuum. Assuming that no physically adsorbed water remains under 10^{-3} mbar vacuum at room temperature, the shift in V_G^+ is likely due to the disappearance of silanol groups on the substrate surrounding the tube. Comparing the V_G^+ shift induced by silanol groups and confined water molecules shows that their impacts are both significant and quantitatively similar. In Fig. S7, we sketch the different adsorption and confinement sites.

Next, we estimate the amount of charge on the nanotube surface induced by the water molecules. Using a simple electrostatic capacitor model, we can write $q_{NT} = C_{eff} V_G$, assuming that the dominant effect of water–nanotube interaction is doping (neglecting capacitance change) and all potential difference is transferred into the charge (neglecting quantum capacitance). Thus, $dq_{NT} = C_{eff}\, dV_G$ relates the charge due to water (dq_{NT}) to the measured neutrality point shift (dV_G). The surface area of the nanotube is $S_{NT} = 2\pi R_{NT} L_{NT}$, where L_{NT} is the length of the nanotube between two successive electrodes, and R_{NT} is the nanotube radius. Assuming R_{NT} = 1 nm and L_{NT} = 5 μm, we calculate ρ_{NT} = 0.06 C m^{-2}. Considering the number of atoms in a nanotube (~2 × 10^{19} atoms per m^2), the charge per carbon atom is approximately ~0.02 e$^-$ per carbon. This value is consistent with previous reports,[24,25] and the negative change suggests OH^- adsorption, as proposed by Grosjean *et al.*[25]

To verify if water–electron coupling depends on the electron density of states (DOS) of the nanotube, we tested two individual open SWCNTs with different metallicities: one semiconducting and the other semi-metallic. We observed the same behavior for both CNTFETs, confirming that the impact of water adsorption is independent of the metallicity of the nanotube (Fig. 3b). Fig. S8 presents the shift in the V_G^+ when several open SWCNTs with different metallicities are exposed to the same environments.

So far, we have focused on individual SWCNTs. We also tested nanotubes in bundles or multi-walled carbon nanotubes (MWCNTs), as identified during the nanotube opening step. When this group of CNTFETs is exposed to different environments (Fig. S9), no significant differences are observed between the open and closed cases. We attribute this behavior to the dominant electronic response of the outermost wall in DWCNTs and MWCNTs, which is not influenced by the presence of water confined inside the central channel. In the case of bundles, it is difficult to distinguish the impact of water due to the diversity of the tubes, varying water adsorption sites, and poor contact with the electrodes. Thus, no clear trend can be drawn from the measurements when the tube is not an individual SWCNT.

To sum up, the impact of water confined inside the CNTFET can be clearly differentiated from that adsorbed outside, but only in the case of individual SWCNTs. The charge transfer observed is independent of the metallicity of the nanotube.

5 Water desorption

We now investigate the desorption of water from an annealed, open CNTFET when exposed to ambient air and varying vacuum levels. Fig. 4 shows the behavior of the transfer characteristic curve as the pressure is decreased stepwise, with measurements taken every 30 minutes until no further change occurs. We measured water desorption on different nanotube lengths (5–25 μm) and various sections (5 μm long) of the same individual open SWCNT.

When examining the impact of water desorption on sections with different lengths (5 μm and 25 μm), we found that all sections behaved qualitatively similarly. A slight decrease in the neutrality point occurred when the pressure was reduced to 10^{-1} mbar, followed by no significant change at 10^{-2} mbar. At 10^{-3} mbar, another slow decrease in V_G was observed. We interpret these stages as follows: the first step at 10^{-1} mbar corresponds to the removal of water molecules physisorbed at the external surface and nearby substrate surfaces, while the second step at 10^{-3} mbar is attributed to the desorption of water molecules confined inside the tube.

The gradual change in V_G during desorption indicates that the removal of both physisorbed and confined water is not instantaneous. Furthermore, the same behavior of the 5 μm and 25 μm sections implies that the desorption mechanism does not depend on the length of the nanotube. Specifically, for water physisorbed outside the tube, desorption is straight-

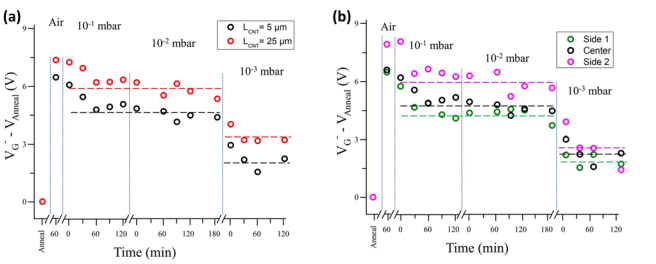

Fig. 4 The change of V_G^- as a function of time for different vacuum pressures. Symbols are experimental data; horizontal and vertical dashed lines are guides to the eye. (a) Water desorption from the CNTFET with different channel lengths (5 μm and 25 μm) of the same individual SWCNT; (b) water desorption from the same channel length (5 μm) of the same individual SWCNT measured near the opened extremities and in the center.

forward. For water confined inside, desorption is governed by the extraction of water molecules and not by the reorganization of the water molecules within the tube. In other words, the primary energy barrier is associated with extracting water from the SWCNT extremities rather than the diffusion of water molecules inside the tube. This is in line with the fact that water confinement is thermodynamically favorable.[3]

The data for various 5 μm sections (Fig. 4b) align with these findings, confirming that the desorption behavior is consistent across the nanotube length. Importantly, no difference was observed between the sections near the opened extremities and those far from them. This further supports the conclusion that the main energy barrier for water molecules during desorption is linked to removal at the SWCNT extremities, not diffusion along the nanotube.

6 Conclusion

We showed that it is possible to differentiate water confined inside an SWCNT from that adsorbed outside, by monitoring the transfer characteristics of a CNTFET based on an individual SWCNT. The water/CNT coupling mechanism was found to be dominated by doping, *i.e.* the charge transfer from the water molecules to the CNT, thanks to the shift of the neutrality point of the transfer characteristics. Water adsorption outside and confinement inside is spontaneous and rather fast (*i.e.* less than 1 min under our experimental conditions), while physically adsorbed water is desorbed in 40–60 minutes at room temperature under vacuum. The impact of water adsorption on the CNT is independent of its metallicity. We identify three water adsorption sites that we attribute to (i) physisorbed water, (ii) water confined inside the CNT, and (iii) chemisorbed water, each with distinct adsorption energy. In addition, we found that the energy barrier for water molecule desorption is governed by their extraction from the SWCNT extremities rather than by their diffusion inside the tube.

Last but not least, our investigation clearly shows that, under our experimental conditions, it was possible to obtain reproducible and reliable outcomes if and only if the CNTFET was made with an individual SWCNT.

Author contributions

A. N., S. P., and F. H. conceived the experiment; S. P. fabricated the samples with the help of Re. J., R. L., E. A., and C. R.; S. P. carried out the experiments with inputs from A. N. and F. H.; N. I. performed the numerical simulation; A. N., F. H., and Ra. J. supervised the work. All authors have read and agreed to the manuscript.

Conflicts of interest

There are no conflicts of interest to declare.

Data availability

The data supporting this article have been included as part of the SI. Supplementary information is available. See DOI: https://doi.org/10.1039/d5nr01939g.

Acknowledgements

We acknowledge the financial support from CNRS-MITI (France) through a 'Momentum' grant. SP acknowledges support from the "State Program 2019–2023" (Azerbaijan) for the Ph.D. scholarship. The work was partly supported by the French Renatech network. AN acknowledges funding from ANR, project number ANR-22-CE09-0004, and funding from the University of Montpellier program 'Soutien à la recherche 2022'. We thank Aloise Degiron for help with Comsol simulations. We thank Saïd Tahir and Vincent Jourdain for help with CNT growth. A CC-BY public copyright license has been applied by the authors to the present document and will be applied to all subsequent versions up to the Author Accepted Manuscript arising from this submission, in accordance with the grant's open access conditions.

References

1 E. Dujardin, T. Ebbesen, H. Hiura and K. Tanigaki, *Science*, 1994, **265**, 1850–1852.
2 G. Hummer, J. Rasaiah and J. Noworyta, *Nature*, 2001, **414**, 188–190.
3 T. A. Pascal, W. A. Goddard and Y. Jung, *Proc. Natl. Acad. Sci. U. S. A.*, 2011, **108**, 11794–11798.
4 L. Fumagalli, A. Esfandiar, R. Fabregas, S. Hu, P. Ares, A. Janardanan, Q. Yang, B. Radha, T. Taniguchi, K. Watanabe, G. Gomila, K. S. Novoselov and A. K. Geim, *Science*, 2018, **360**, 1339–1342.
5 D. Cao, P. Pang, J. He, T. Luo, J. H. Park, P. Krstic, C. Nuckolls, J. Tang and S. Lindsay, *ACS Nano*, 2011, **5**, 3113–3119.
6 W. Kim, A. Javey, O. Vermesh, Q. Wang, Y. Li and H. Dai, *Nano Lett.*, 2003, **3**, 193–198.
7 I. Heller, J. Männik, S. G. Lemay and C. Dekker, *Nano Lett.*, 2009, **9**, 377–382.
8 X. Cui, M. Freitag, R. Martel, L. Brus and P. Avouris, *Nano Lett.*, 2003, **3**, 783–787.
9 H. G. Ong, J. W. Cheah, X. Zou, B. Li, X. H. Cao, H. Tantang, L.-J. Li, H. Zhang, G. C. Han and J. Wang, *J. Phys. D: Appl. Phys.*, 2011, **44**, 285301.
10 T. Sharf, J. W. Kevek, T. DeBorde, J. L. Wardini and E. D. Minot, *Nano Lett.*, 2012, **12**, 6380–6384.
11 I. Heller, A. M. Janssens, J. Männik, E. D. Minot, S. G. Lemay and C. Dekker, *Nano Lett.*, 2008, **8**, 591–595.
12 R. Pati, Y. Zhang, S. K. Nayak and P. M. Ajayan, *Appl. Phys. Lett.*, 2002, **81**, 2638–2640.
13 T. Someya, P. Kim and C. Nuckolls, *Appl. Phys. Lett.*, 2003, **82**, 2338–2340.

14 M. E. Roberts, M. C. LeMieux and Z. Bao, *ACS Nano*, 2009, **3**, 3287–3293.
15 H. Lin and S. Tiwari, *Appl. Phys. Lett.*, 2006, **89**, 073507.
16 P. R. Mudimela, K. Grigoras, I. Anoshkin, A. Varpula, V. Ermolov, A. Anisimov, A. Nasibulin, S. Novikov and E. Kauppinen, *J. Sens.*, 2012, **2012**, 496546.
17 C. Lee and M. Strano, *Langmuir*, 2005, **21**, 5192–5196.
18 D. R. Kauffman and A. Star, *Angew. Chem., Int. Ed.*, 2008, **47**, 6550–6570.
19 P. S. Na, H. Kim, H.-M. So, K.-J. Kong, H. Chang, B. H. Ryu, Y. Choi, J.-O. Lee, B.-K. Kim, J.-J. Kim and J. Kim, *Appl. Phys. Lett.*, 2005, **87**, 093101.
20 V. Jourdain and C. Bichara, *Carbon*, 2013, **58**, 2–39.
21 Y.-X. Lu, C.-T. Lin, M.-H. Tsai and K.-C. Lin, *Micromachines*, 2022, **13**, 509.
22 X. Wei, Q. Chen, Y. Liu and L. Peng, *Nanotechnology*, 2007, **18**, 185503.
23 S. Khasminskaya, F. Pyatkov, B. S. Flavel, W. H. Pernice and R. Krupke, *Adv. Mater.*, 2014, **26**, 3465–3472.
24 M. Manghi, J. Palmeri, F. Henn, A. Noury, F. Picaud, G. Herlem and V. Jourdain, *J. Phys. Chem. C*, 2021, **125**, 22943–22950.
25 B. Grosjean, M.-L. Bocquet and R. Vuilleumier, *Nat. Commun.*, 2019, **10**, 1656.